Available online at www.sciencedirect.com

ScienceDirect

Procedia Structural Integrity 33 (2021) 695–703

Structural Integrity Procedia

www.elsevier.com/locate/procedia

IGF26 - 26th International Conference on Fracture and Structural Integrity

Notch Effect in the Tensile Quasi-Static Behaviour of 40% Short Glass Fibre - PPS Reinforced Composites

Mauro Ricotta[a]*, Marco Sorgato[a], Michele Zappalorto[b]

[a]*University of Padova, Department of Industrial Engineering, Via Venezia, 1, 35131 Padova, Italy*
University of Padova, Department of Management and Engineering, Stradella San Nicola 3 – 36100 Vicenza, Italy

Abstract

The quasi-static tensile behaviour of notched and unnotched specimens made of 40% wt. glass fibre-Polyphenylenesulphide (40GF-PPS) short fibre reinforced composite has been investigated in this work.
Plain and notched specimens (with notch radius ranging from 0.25 mm to 10 mm) were manufactured with two different fibre orientation angles (0° and 90°) and tested under tension loadings with the aim to understand the effect of the notch root radius and the notch geometry. Contemporaneously, a careful analysis was carried out both at the macroscopic and microscopic level, discussing the analogies existing between plain and notched specimens.

Keywords: Short Fibre Reinforced Composites; Notch effect; Polyphenylenesulphide, Static Notch sensitivity.

1. Introduction

Polyphenylenesulphide (PPS) is a linear semi-crystalline thermoplastic polymer with repeated thiophenyl units and is widely used in structural applications offering good high temperature resistance, chemical resistance and dimensional stability. Moreover, thanks to its low viscosity, PPS can be moulded with high percentages of fillers and reinforcements, which are able to significantly reduce the material inherent brittleness. These fillers and reinforcements can increase the material strength, surface properties, dimensional stability and electrical properties.

* Corresponding author. Tel.: +39-049-827-6762; fax: +39-049-827-6785.
E-mail address: mauro.ricotta@unipd.it

10.1016/j.prostr.2021.10.077

Therefore, PPS-SFRCs are widely used to manufacture structural components for the automotive and aerospace fields. In view of this, several papers can be found in the open literature concerning the load bearing characteristics of short fibre reinforced PPS composites, as Karger-Kocsis et al (1987), Lou et al (1988), Zhang et al (1993), Vieille et al (2011), Vieille et al (2016).

To the authors' knowledge, comparatively far less attention was devoted to the quasi-static tensile and compressive strength of notched GF-PPS *short fibre* reinforced composites (see Yilmaz et al (2007), Ricotta et al (2021)).

In the present paper, the tensile static strength of GF-PPS SFRCs in the presence of notches is investigated, with the main aim to provide new experimental results useful for engineers involved in the structural design with SFRCs and to understand the effect of the stress concentration, the loading condition and the fibre orientation angle on the damage mechanisms and the overall strength. In view of this, specimens having different notch geometries and fibre orientations were milled starting from 40% wt. short glass fibre-PPS reinforced injection moulded plates. The choice of obtaining the specimens from an injection moulding plaque, instead of directly moulding them, was driven by the common-practice in Industry of machining small features on SFRCs when high accuracy and precision are required, as reported by Kuram (2016). Later on, quasi-static tensile tests were carried out on the manufactured specimens with the aim to carefully study the notch sensitivity, the effect of the notch root radius and the fibre orientation angle. Taking advantage of a digital microscope and a Scanning Electron Microscope (SEM), the damage analysis was carried out, investigating the damage mechanisms, to better understand and explain the significant effect of the above-mentioned parameters on the strength of notched components.

2. Material, specimen geometry and test methods

The investigated material was a short fibre reinforced Polyphenylenesulphide, containing 40 % wt. glass fibres with a nominal diameter of 10 μm (designation: GF40-PPS), provided by Solvay.

Quasi-static tensile tests were carried out on plain and notched specimens, obtained by machining injection moulded 200 mm × 200 mm plates, with 1.8 -mm-thick (see Fig. 1a). Specimens were manufactured taking advantage of a Battenfeld HM 180/525H/210 S injection moulding machine and using the process conditions reported in Table 1. Plain specimens were machined out by milling at three orientation angles θ=0°, 45° and 90° as reported in Fig. 1a.

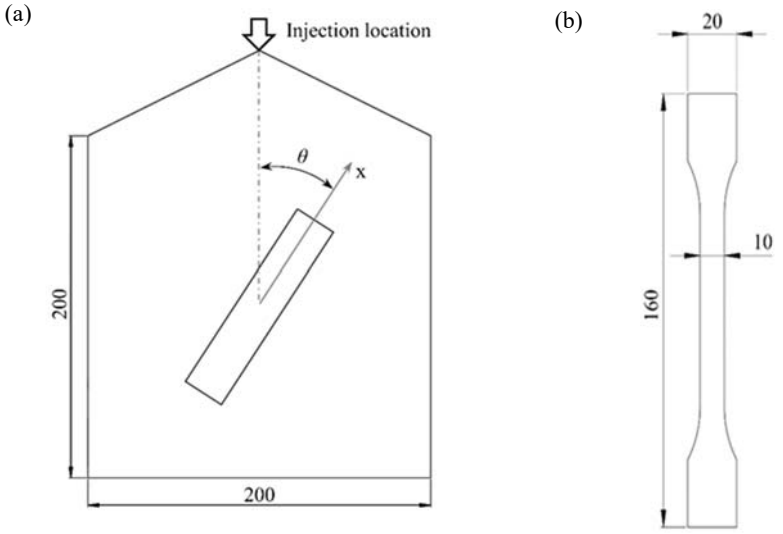

Fig. 1. (a) Schematization of the injection moulded plate from which different specimens at different orientation (θ) were obtained; (b) Specimen geometry of plain material. Specimen thickness t=1.80 mm

Table 1. Injection moulding process parameters

Mould temperature [°C]	80
Melt temperature [°C]	310
Flow rate [cm^3/s]	40
Packing pressure [bar]	850
Packing time [s]	21

The residual fibre length after the injection moulding process, was evaluated by placing in an oven three specimens at a temperature of 700 °C for 1 hour, to burn off the polymer matrix. Then, a small portion of the fibres was dispersed in demineralized water by an ultrasound separator and dried. These samples were analysed using an optical Coordinate Measurement Machine (CMM), Werth Video-Check IP 400. Finally, the length of about 100 fibres was measured according to the procedure described in Berton et al (2010).

The quasi-static tests were conducted on a servo-hydraulic MTS 858 Mini Bionix II machine equipped with a 15 kN load cell. The tensile properties of the plain material were measured by carrying out quasi-static tests (based on ISO 527 standard) on specimens machined according to the geometry shown in Fig. 1b, imposing a crosshead speed of 2 mm/min. At least three static tests were carried out for each fibre orientation and a MTS 634.12-24 extensometer with a gauge length of 25 mm was adopted for measuring the elastic modulus.

Notched specimens, instead, were milled to obtained the geometries shown in Fig. 2, by using an ultra-precise milling centre Kugler Micromaster 5X to avoid the influence of geometrical features on the polymer flow, which can generate weld lines or non-uniform fibre distribution. In more details, lateral rounded V notched specimens with an opening angle of 90° were used, varying the notch depth from 2 mm to 10 mm and the notch root radius from 0.25 mm to 5 mm; in addition, lateral symmetrical semi-circular notches were considered with R=10 mm. Finally, the fracture surfaces of plain and notched specimens were analysed by using a QUANTA 450 FEI scanning electron microscope.

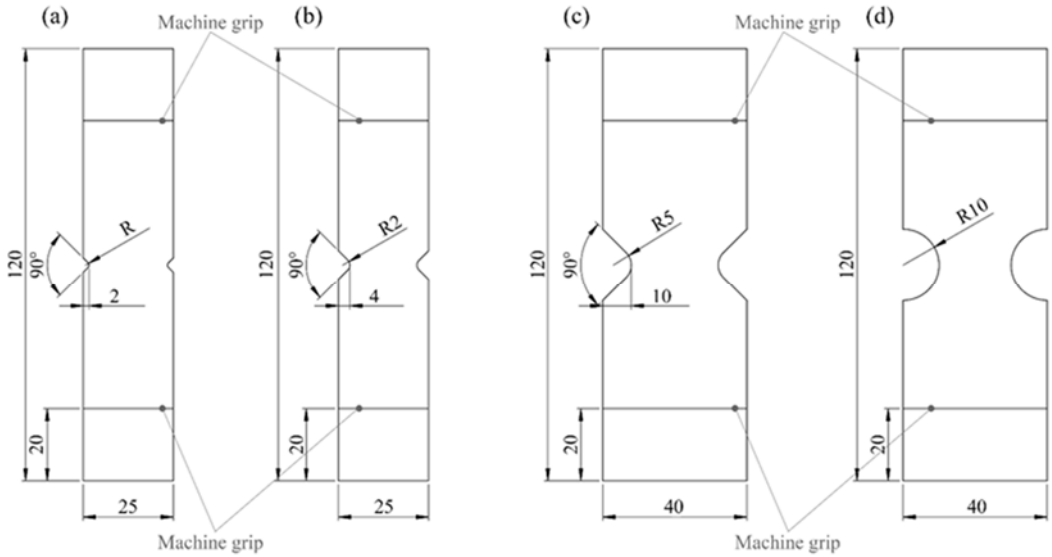

Fig. 2. Geometries of notched specimens adopted for tensile static tests: (a) R=0.25 mm, R=0.50 and R=1 mm

3. Experimental results

The fibre length distribution is illustrated in Fig. 3a, where the fibre lengths are plotted, divided into 0.4 mm-classes against their frequency. It can be observed that the majority of fibre lengths ranged between 0.16 mm and 0.24 mm. Quantitative measurements of the residual fibre length were performed, obtaining a Weight Average Fibre Length (WAFL) equal to 0.226 mm and an average fibre diameter equal to 12 μm. Finally, the through-the-thickness Fibre Orientation (FO) was evaluated, by analysing the transversal section of specimens by means of the SEM and, as expected, the typical skin-core morphology was observed: in detail, the core had a thickness approximately equal to 0.15 mm, corresponding to 8.3% of the entire section.

3.1 Tensile tests on plain specimens

Fig. 3b shows the engineering stress-engineering strain curves, obtained by carrying out the tensile tests on plain specimens. As expected, the ultimate tensile strength σ_{UTS} decreases as the orientation angle increases. The same trend was observed for the ultimate tensile strain, ε_{UTS}. The average values of the elastic and mechanical properties are listed in Table 2.

The elastic properties in the material reference system E_1, E_2 and G_{12} were estimated from the measured values of the tensile modulus E_x, applying the theory of linear elasticity for orthotropic materials, as proposed by De Monte et al (2010), according to which E_x can be expressed as a function of the orientation angle θ:

$$E_x(\theta)=\left[\frac{\cos^4\theta}{E_1}+\frac{\text{sen}^4\theta}{E_2}+\frac{1}{4}\left(\frac{1}{G_{12}}-\frac{2\nu_{12}}{E_1}\right)\text{sen}^2\theta\right]^{-1} \quad (1)$$

The experimental elastic properties reported in Table 2 were fitted according to Eq. (1), by using the least square fitting algorithm and considering E_1, E_2 and G_{12} as parameters; the Poisson ratio ν_{12} was assumed to be $\nu_{12} = 0.40$, as proposed by Ricotta et al (2021). The calculated E_1, E_2 and G_{12} values are listed in Table 3. The out-of-plane elastic properties, to be used in the Finite Element (FE) analyses described later, were defined according to the engineering assumption that $E_2=E_3$, $G_{13}=G_{12}$ and $\nu_{13} = \nu_{12}$ (see De Monte et al, 2010). Finally, the values of G_{23} and ν_{23} were set as equal of those of the PPS matrix, assuming the out of plane behaviour to be matrix-dominated.

Table 2. Static strength properties of unnotched 40% wt GF-PPS short fibre reinforced composites

Fibre orientation [deg]	E_x [MPa]	σ_{UTS} [MPa]	ε_{UTS} [%]
0	14780	174.4	1.71
45	8760	93.4	1.41
90	7490	64.9	1.00

Table 3. Elastic properties from theory of elasticity for 40% wt GF-PPS short fibre reinforced composites

E_1 [MPa]	E_2 [MPa]	E_3 [MPa]	G_{12} [MPa]	G_{13} [MPa]	G_{23} [MPa]	ν_{12}	ν_{13}	ν_{23}
14780	7490	7490	3230	3230	1400	0.40	0.40	0.37

3.2 Tensile tests on notched specimens

The results of the quasi-static tensile tests on notched specimens are first presented considering the load-displacement curves. The macroscopic behaviour of the notched specimens with θ=0° and θ=90° is presented in Fig.4a and Fig. 4b, respectively, where a limited amount of non-linearity can be noted for both the orientation angles.

Therefore, it can be concluded that a brittle and quasi-brittle macroscopic behaviour characterises the quasi-static tensile tests on notched specimens, as also noted by Vielle et al (2011) and Vielle et al (2016).

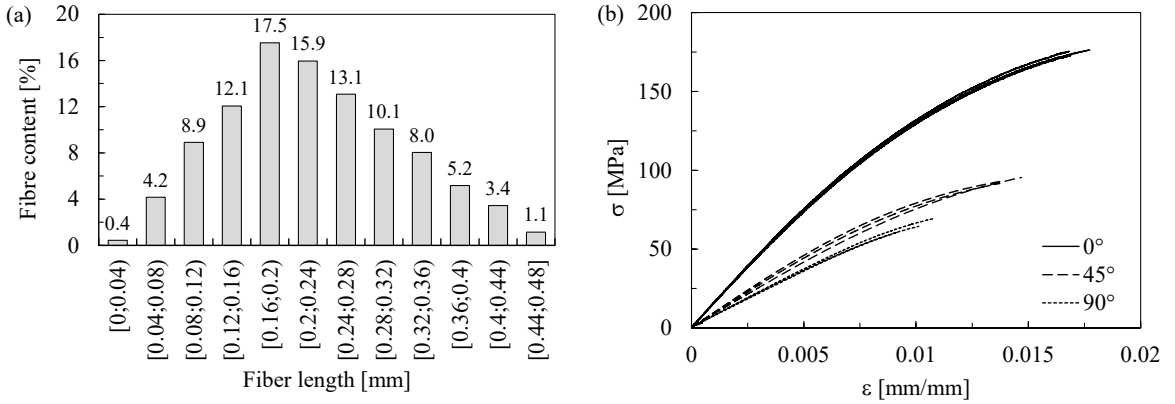

Fig. 3. (a) Fibre length distribution and (b) engineering stress-engineering strain curves of unnotched GF40-PPS specimens.

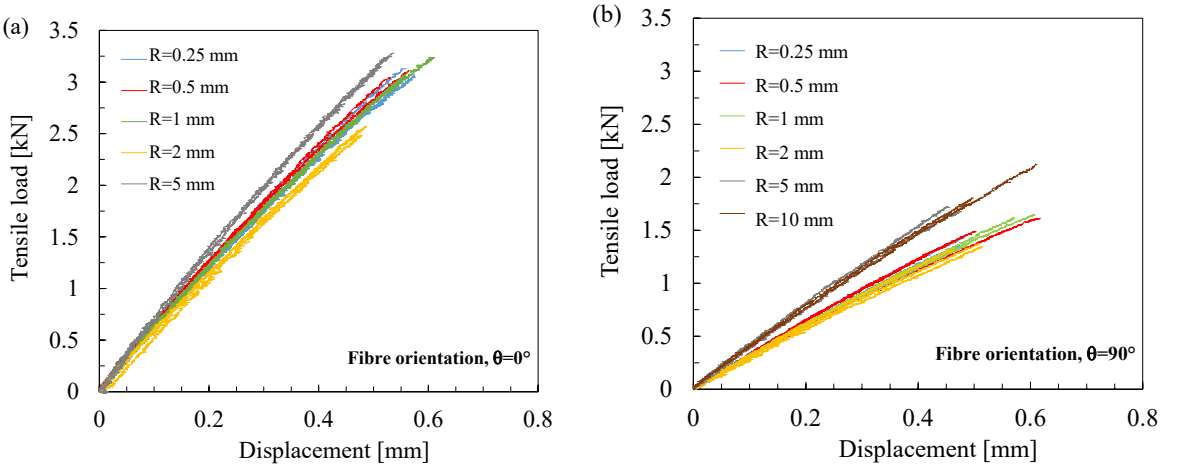

Fig. 4. Tensile load-displacement curves for notched (a) θ=0° and (b) θ=90° specimens.

The theoretical stress concentration factors referred to the net section, K_{tn}, relevant to the notched geometries were calculated through 3D linear elastic finite element analyses carried out with the commercial software ANSYS®, by using 8-node SOLID185 elements along with the elastic material properties listed in Table 3. To account for the machine grip effect in the numerical models, displacements were applied to the lines highlighted in Fig. 2.

The results of the quasi static tests carried out on notched geometries were reanalysed in terms of ultimate tensile net-stress strength, $\sigma_{n,UTS}$, calculated by simply dividing the ultimate applied load by the net-area of the specimen, and they are plotted against K_{tn} in Fig. 5a and 5b for θ=0° and θ=90°, respectively. In the same figures, the following two limiting conditions are also reported:

i. on the left-hand side, the asymptote corresponding to a full notch sensitivity condition, according to which the static strength of notched geometries is estimated dividing the material strength by the theoretical stress concentration factor, σ_{UTS}/K_{tn};

ii. on the right-hand side, the asymptote corresponding to the strength of the sharp V (zero root radius) notch, σ_{UTS}^{V}, which was estimated as the strength of the V notch case with R=0.25 mm. This last-mentioned choice is fully justified by the fact that the region in front of the notch tip, where the stress distribution of the rounded notch with R=0.25 mm significantly differs from that of the corresponding sharp V (zero root radius) notch has a very limited

extension (see Ricotta et al (2021)). According to Zappalorto (2020), the size of this region can be estimated as d_L=0.016 mm for θ=0° and d_L=0.029 mm for θ=90°.

The two asymptotes intersect at a given K_{tn} value, K^*_{tn}, that can be estimated as:

$$K^*_{tn} = \frac{\sigma_{UTS}}{\sigma^V_{UTS}} \tag{2}$$

Fig. 5 shows that for both the orientation angles, larger notch radii lead to higher $\sigma_{n,UTS}$, as also observed by Toll et al. (1992) and Potti et al. (2000) for short glass fibre/polyamide 66 composites and in Hitchen et al (1994) for short carbon fibre/epoxy composites. Moreover, one can see that both for θ=0° and θ=90° the strength of notched specimens is always comprised between the strength of the relevant plain material, σ_{UTS} (notch insensitivity condition) and the value σ_{UTS}/K_{tn} (full notch sensitivity condition). Finally, for K_{tn} values larger than K^*_{tn}, the experimental data related to notched components tend toward the strength of the pointed V notch case, σ^V_{UTS}. This behaviour is more evident for specimens with θ=0° than for those with θ=90°, and this result will be later justified considering the damage mechanisms. Moreover, as shown in Fig. 5, within a certain degree of accuracy, the trend of the experimental data can be approximated using the following Aysmptotic Matching equation based on the two asymptotes above described:

$$\sigma_{n,UTS} = \frac{\sigma_{UTS}}{\left\{\left[(K_t - 1)^{-m} + (K^*_{tn} - 1)^{-m}\right]^{-1/m} + 1\right\}} \tag{3}$$

where m is a matching coefficient controlling the transition from one asymptote to the other. According to Zappalorto (2019), values of m comprised between 1.25 (brittle behaviour) and 3 (ductile behaviour) are expected to fit well with experimental results. In this work, m=2 and m=1.25 were used for θ=0° and θ=90°, respectively, to obtain the trends of Fig. 5.

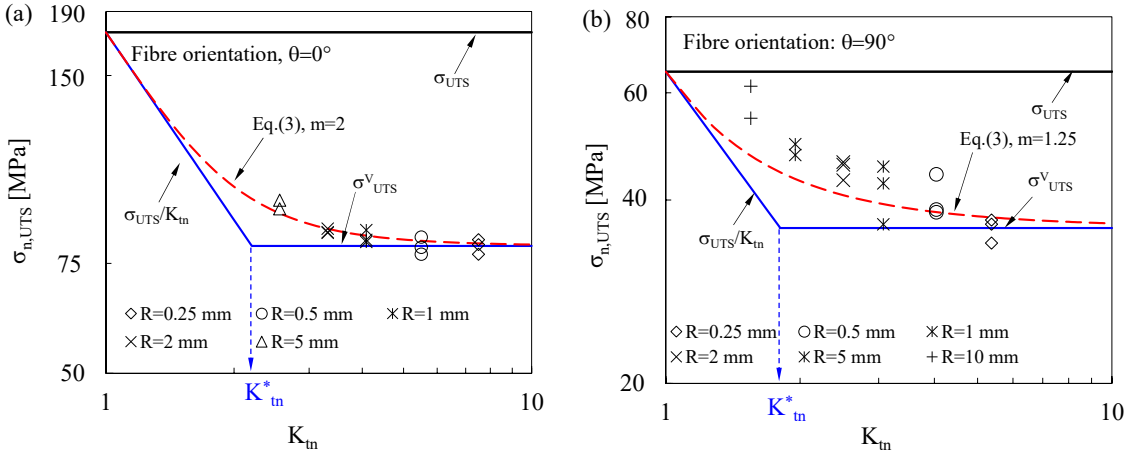

Fig. 5. Results of tensile static tests carried out on (a) 0° and (b) 90° notched specimens.

A summary of all the experimental data in terms of Generalised Stress Intensity Factors (GSIFs) is presented in figure 6. The orthotropic GSIF has been calculated according to the expression (see Zappalorto, 2019, for more details):

$$K_{1\rho} = M \cdot \sigma_{tip} r_0^{1-\lambda_1} \tag{4}$$

where σ_{tip} is the notch tip stress, λ_1 is the linear elastic stress eigenvalue and r_0 can be determined as:

$$r_0 = \frac{\pi - 2\alpha}{2\pi - 2\alpha} R \tag{5}$$

In particular, the following equation was found to well correlate with the experimental data (Ricotta et al. 2021):

$$\frac{K_{1\rho c}}{K_{1c}} = \left\{ 1 + \left(\frac{R}{R_N} \right)^{\kappa(1-\lambda_1)} \right\}^{\frac{1}{\kappa}} \tag{6}$$

where K_{1c} is the GSIF value of the pointed V-notch and R_N is the notch root radius giving the transition from a full notch sensitivity (for radii larger than R_N) to an incomplete notch sensitivity (for radii smaller than R_N) and can be determined according to the following expression (Zappalorto, 2019):

$$R_N = \frac{q}{q-1} r_{0N} = \frac{q}{q-1} \left(\frac{1}{M} \frac{K_{1c}}{\sigma_0} \right)^{\frac{1}{1-\lambda_1}} \tag{7}$$

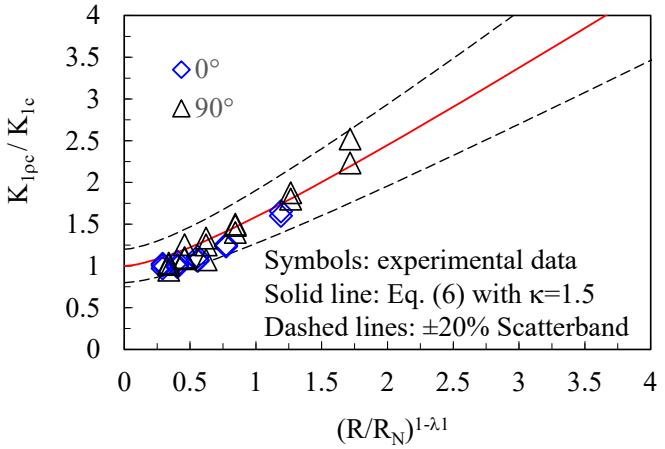

Fig. 6. Critical GSIF of SFC notched components. Comparison between the predictions based on Eq. (6) and experimental data.

4. Damage analysis

The microscopic damage mechanisms frequently observed in the case of θ=0° orientation angle are shown in Fig. 7a, where multiple broken fibres can be noted and a considerable presence of fibre pull-outs (see the approximately circular marks in the matrix), as also observed by Zhang et al (1993) for CF-PPS composites. Moreover, profuse crazing is evident in the matrix in the plane normal to the applied stress, close to the fibre end, that can be located a posteriori, considering the circular marks visible in the matrix. A different damage scenario was found in the case of θ=90° orientation angle, as shown in Fig. 7b, where, indeed, multiple initiation and growth of hackles from the fibre tracks can be clearly observed, as usually found in the case of brittle matrices, as reported by Hayes et al (2015).

Typical evidences of the damage observed close to the notch tip of V-notched specimens with θ=0° are reported in Fig. 8a, which refers to R=0.25 mm and a= 2 mm, as an example. As evident, a quite extensive presence of broken fibres, fibre-matrix debonding and fibre pull-out can be observed as well as craze formation and fibrillation induced by the PPS matrix ductility, as for the plain specimens. Regarding the specimens with θ=90°, matrix failure and formation of hackles were noticed, as shown in the pictures in Fig. 8b, taken from the notch tip of a V-notched specimen with R=5 mm and a = 10 mm, suggesting that the cracks propagated mainly at the fibre-matrix interface. It is also worth mentioning that for all the tested specimen geometries the same damage mechanisms were observed.

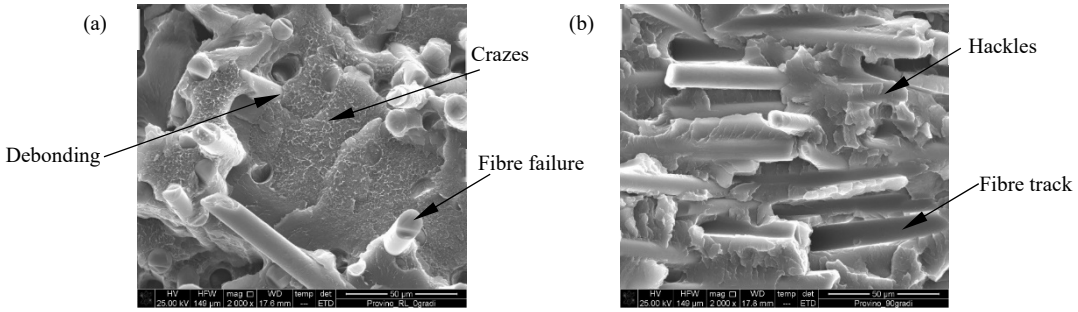

Fig. 7. Characteristic fracture surface observed for (a) θ=0° and (b) θ=90° specimens failed during a tensile test.

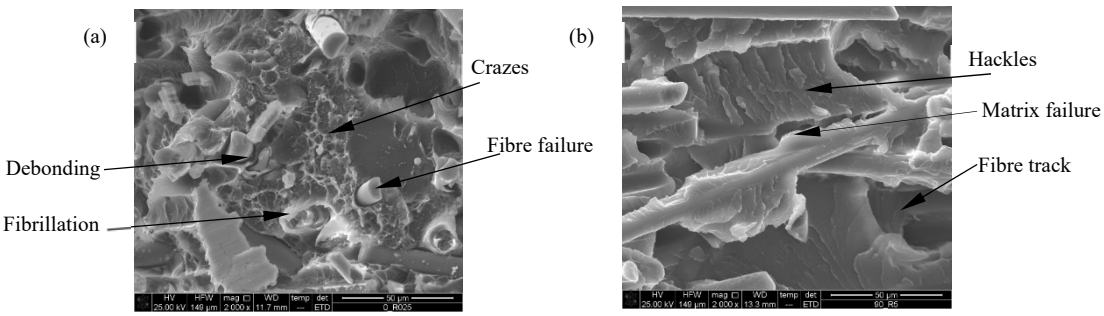

Fig. 8. Characteristic fracture surface and damage mechanisms observed for (a) θ=0° V-notched specimen with R=0.25 mm and a= 2 mm, (b) θ=90° V-notched specimen with R=5 mm and a = 10 mm.

In the light of this body of experiments, it can be concluded that in the region close to the tip of notched specimens with θ=0°, several energy-absorbing damage mechanisms were observed, namely fibre failure, fibre-matrix debonding, fibre pull-out, craze formation and fibrillation, which contributed to the toughening of the PPS matrix. Differently, as also observed by Agarwal et al (1990), comparatively far less energy-absorbing mechanisms were noted close to the tip of notched specimens with θ=90°, so that the toughening effect induced by the fibres is limited, and the overall composite behaviour is more controlled by the brittleness of the matrix. This difference in terms of damage mechanisms supports that observed in terms of macroscopic mechanical response shown in Fig. 5 and it can be noted that:

- in regard to the specimens with θ=0° (Fig. 7a), almost independently of the notch root radius, most of the notched specimens exhibited the same strength of the corresponding sharp (zero root radius) V-notch. This can be indeed associated to a pronounced dissipation zone ahead of the notch tip;
- in regard to the specimens with θ=90° (Fig. 7b), it is evident that almost all the experimental data are in the transitional region comprised between the sharp (zero root radius) V-notch strength (incomplete notch sensitivity) and the value σ_{UTS}/K_{tn} (full notch sensitivity). This can be indeed associated to a brittle or quasi-brittle behaviour (see Fig. 4b), with a limited dissipation zone ahead of the notch tip.

5. Conclusions

The static tensile strength of notched and plain 40% wt. glass fibre- Polyphenylenesulphide (40GF-PPS) short fibre reinforced composite was analysed experimentally and the associated damage mechanisms were investigated. To this end, plain and notched specimens (with notch radius ranging from 0.25 mm to 10 mm and notch depth ranging from 2 to 10 mm) were manufactured with two different fibre orientation angles (as measured with respect to the loading direction), namely θ=0° and θ=90°. Concerning the plain material, different damage mechanisms were observed depending on the fibre orientation angle. In particular, in the case of θ=0°, fibre failure, fibre pull-out and profuse

crazing in the plane normal to the applied stress were observed, whilst for θ=90° the damage scenario was characterised by the growth of hackles from the fibre tracks present on the matrix. Regarding the notched specimens, it was observed that the larger the notch radius, the higher the static strength is, for both the orientation angles. Moreover, an incomplete notch sensitivity was noted, according to which the strength of notched specimens was always comprised between the strength of the relevant plain material, σ_{UTS} (notch insensitivity condition), and the value of the ratio σ_{UTS}/K_{tn} (full notch sensitivity condition). Concerning the notched geometries, a $K^*_{tn} = \sigma_{UTS} / \sigma^V_{UTS}$ value was defined such that for notched geometries with $K_{tn} > K^*_{tn}$, their static strength tends toward the strength of the pointed V notch case, σ^V_{UTS}. This behaviour is more evident for notched specimens with θ=0°, for which pronounced energy absorbing mechanisms were noted close to the notch tip. Finally, the damage analysis carried out at the microscopic level showed that the damage mechanisms observed in the notched specimens are equal to those noted in the relevant unnotched material.

References

Agarwal, B.D., Broutman, L.J., 1990. Analysis and performance of fibre composites. John Wiley & Sons, Inc, Toronto.

Berton, M., Cellere, A., Lucchetta, G., 2010. A new procedure for the analysis of fibre breakage after processing of fibre-reinforced thermoplastics, International Journal of Material Forming 3, 671-674.

De Monte, M., Moosbrugger, E., Quaresimin, M., 2010. Influence of temperature and thickness on the off-axis behaviour of short glass fibre reinforced polyamide 6.6 – Quasi-static loading. Composites Part A-Applied Science 41, 859-871.

Hayes, M.D., Edwards, D.B., Shah, A.R., 2015. Fractography in failure analysis of polymers. PDL Handbook Series, Elsevier.

Hitchen, S.A., Ogin, S.L., Smith, P.A., Soutis, C., 1994. The effect of fibre length on fracture toughness and notched strength of short fibre/epoxy composites. Composites 25, 407-413

ISO 527 Standard, 2019. Plastics - Determination of tensile properties, International Organization for Standardization.

Karger-Kocsis, J., Friedrich, K., 1987. Microstructural details and the effect of testing conditions on the fracture toughness of injection-moulded poly(phenylene-sulphide) composites. Journal of Material Science 22, 947-961.

Kuram, E., 2016. Micro-machinability of injection molded polyamide 6 polymer and glass-fiber reinforced polyamide 6 composite. Composirtes Part B-Engineering 88, 85-100

Lou, A.Y., Murtha, T.P., 1988. Environmental effects on glass fiber reinforced pps stampable composites. Journal of Materials Engineering 10, 109-116.

Potti, P.K.G., Rao, B.N., Srivastava, V.K., 2000. Notched tensile strength for long- and short-fiber reinforced polyamide. Theoretical and Applied Fracture Mechanics 33, 145-152.

Ricotta, M., Sorgato, M., Zappalorto, M., 2021. Tensile and compressive quasi-static behaviour of 40% short glass fibre - pps reinforced composites with and without geometrical variations. Theoretical and Applied Fracture Mechanics 114, 102990.

Ryton® R-4-200NA. https://www.solvay.com/en/products/brands/ryton-pps datasheet.

Toll, S., Aronsson, C. G., 1992. Notched strength of long- and short-fibre reinforced polyamide. Composites Science and Technology 45, 43-54.

Vieille, B., Taleb, L., 2011. About the influence of temperature and matrix ductility on the behavior of carbon woven-ply PPS or epoxy laminates: Notched and unnotched laminates. Composites Science and Technology 71, 998-1007.

Vieille, B., Chabchoub, M., Bouscarrat, D., Keller. C., 2016, Prediction of the notched strength of woven-ply PolyPhenylene Sulfide thermoplastic composites at a constant high temperature by a physically-based model. Composite Structures 153, 529-537.

Yılmaz, T., Sınmazcelik, T., 2007. Geometric parameters and chemical corrosion effects on bearing strength of polyphenylenesulphide (PPS) composites. Materials and Design 28, 1695-1698.

Zhang, M., Zeng, H., Zhang, L., Lin, G., Li, R.K.Y., 1993. Fracture characteristics of discontinuous carbon fibre-reinforced PPS and PES-C composites. Polymers and Polymer Composites 1, 357-365.

Zappalorto, M., 2019. Mode I Generalised Stress Intensity Factors for rounded notches in orthotropic plates. Theoretical and Applied Fracture Mechanics 101, 356-364.

Zappalorto, M., 2020. Universal equations for the mode I stress distribution in finite size orthotropic plates with blunt notches and holes, Theoretical and Applied Fracture Mechanics 109, 102768